ACS OMEGA

http://pubs.acs.org/journal/acsodf

Article

Synthetic versus Natural Precursor Layer: A Study on the Properties of Biocompatible Chitosan/Carboxymethyl Cellulose Nanofilms

Juraj Nikolić,* Ana Ivančić, Tin Klačić, and Davor Kovačević*

Cite This: *ACS Omega* 2023, 8, 20031−20041

Read Online

ACCESS | Metrics & More | Article Recommendations | Supporting Information

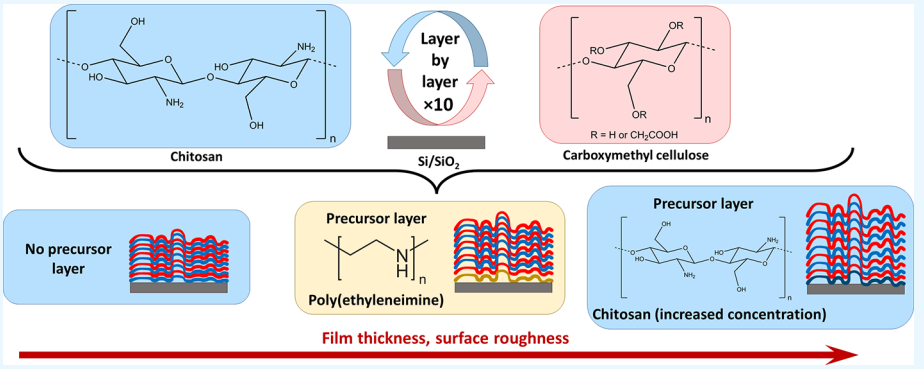

ABSTRACT: Polyelectrolyte multilayers are nanofilms with vast applications in numerous areas such as medicine and food industry. Recently, they have been getting a lot of attention as potential food coatings for the prevention of fruit decay during transportation and storage, and therefore the coatings need to be biocompatible. In this study, we fabricated thin films made of biocompatible polyelectrolytes, positively charged polysaccharide chitosan, and negatively charged carboxymethyl cellulose on a model silica surface. Typically, to enhance the properties of the prepared nanofilms, the first layer (precursor layer) of poly(ethyleneimine) is used. However, for the construction of completely biocompatible coatings, this could be problematic due to potential toxicity. This study offers an option for a viable candidate as a replacement precursor layer: chitosan itself was adsorbed from a more concentrated solution. In the case of chitosan/carboxymethyl cellulose films, using chitosan over poly(ethyleneimine) as a precursor layer has shown a twofold increase in film thickness, as well as an increase in film roughness. In addition, these properties can be tuned by the presence of a biocompatible background salt (e.g., sodium chloride) in the deposition solution that has proven to change the film thickness and surface roughness depending on the salt concentration. Such a straightforward way of tuning the properties of these films combined with their biocompatibility makes this precursor material a prime candidate for use as a potential food coating.

1. INTRODUCTION

The longevity of stored and transported food is a global problem that is exacerbated by supply chain disruptions due to either predictable or unforeseen environmental issues and societal events. This problem particularly affects low-shelf-life food, like fruits and vegetables, due to their need to be transported long distances before reaching final consumers. The primary causes of the low longevity of these products are bacterial and fungal-caused rot which occurs due to various environmental reasons. To battle this phenomenon, food protection plays an essential role in its long-term preservation, and different kinds of materials have been studied to this effect.[1−5]

One of the more successful materials in this ongoing pursuit is a class of thin films called polyelectrolyte multilayers (PEMs).[6] These films are formed on a solid surface via electrostatic interactions, hydrogen bonding, covalent bonding, or biospecific interactions between the components of the film, polycations, and polyanions.[7,8] Their properties depend on the type of substrate and the type of polycation/polyanion pair and are also dependent on various adsorption conditions.[8−13] Typically, the most easily adjustable adsorption conditions are deposition time, polyelectrolyte concentration, pH, and ionic strength or the type of salt added. For instance, it is well known that for electrostatically bonded multilayers, an increase in ionic strength leads to an increase in film thickness.[14,15] On the other hand, Schlenoff and co-workers showed that if the polyelectrolyte multilayers are assembled based on hydrogen

Received: April 5, 2023
Accepted: May 11, 2023
Published: May 25, 2023

ACS Publications

© 2023 The Authors. Published by American Chemical Society

bonding, the thickness decreases with the ionic strength and eventually reaches a plateau at a high salt concentration.[16] In addition to these experimental parameters, the presence of the first layer, often called a precursor or an anchoring layer, plays an important role. Usually, poly(ethyleneimine) (PEI) in its various forms is used as the precursor layer for multilayer buildup to enhance its properties.[17−19] However, its toxicity to both bacterial and, especially, human cells is a cause for concern for its application in food coatings.[20−23]

PEMs can be fabricated in such a way that they inherit the properties of their components and as such can be specifically designed. Currently, many studies have proven that chitosan (CS), a natural polycation derived from chitin, is one of the main components in a large slew of composite-like materials which have great potential for wide application in the food industry.[24−26] The main highlights of chitosan are its abundance, antibacterial and antifungal properties, and the fact that it is a nontoxic and environmentally friendly compound.[27] Until now, chitosan has been combined with a great deal of other materials such as essential oils,[2,3] polyanions,[9,28,29] and even metal oxides[27] forming cocrystals,[30] films,[31] and different types of coatings or complexes[9,10,29,32−34] with various applications in food industry[1,26,35,36] and medicine technology.[28,37,38] As the formation of PEMs requires both a polycation and a polyanion, chitosan had to be paired with a suitable biocompatible and nontoxic polyanion. Until now, multiple polyanions fall into this category.[39−41] For our study, we chose carboxymethyl cellulose (CMC), a derivative of naturally occurring cellulose. Among multiple other desirable properties, CMC is easily synthesized from cellulose; it is widely available and has a broad range of applications as a biocompatible polymer.[42] In addition, studies on CS/CMC materials have shown that this system displays self-healing properties that would be very desirable for the longevity of CS/CMC multilayers.[43,44] Even though CS and CMC are biocompatible polymers, many of the mentioned studies also add PEI as the precursor layer to create thicker and more durable PEMs, but its potential toxicity is a cause of concern for the applications of such materials.

The goal of this study was to provide an alternative, biocompatible, and environmentally safe precursor layer for the preparation of polyelectrolyte nanofilms for application in the food industry, in contrast to, the current mainstream, PEI. Moreover, we additionally studied the effect of the addition of sodium chloride, another biocompatible compound, on the surface properties of all examined nanofilms. The main methods used in this study were ellipsometry for monitoring the film growth and atomic force microscopy (AFM) which was used to determine the surface morphology, film thickness, and roughness.

2. EXPERIMENTAL SECTION

2.1. Substrate. Polished silicon (Si) wafers of 1 × 1 cm^2 size and 0.675 mm thickness (⟨100⟩ orientation, P-doped with boron) were cut from larger plates (Siltronic AG) for PEM preparation, ellipsometry measurements, and atomic force microscopy. Afterward, the Si wafers were cleaned with "piranha" solution (3:1 mixture of concentrated H_2SO_4 and 30% H_2O_2 solution, purchased from Gram-mol and Merck, respectively; *WARNING: "Piranha" solution is a highly corrosive and a powerful oxidizing agent and should be handled with great care*) for 1 h, rinsed with deionized water, dried with a stream of argon gas (Argon 5.0, Messer), and stored under ambient conditions in a well-sealed plastic container. It should be noted that a thin oxide layer (SiO_x) is spontaneously formed by the oxidation of Si with oxygen from air and is reported to be around 2 nm thick.[11] Deionized water used in all experiments was prepared in a three-stage Millipore Milli-Q Plus 185 purification system which had an initial conductivity lower than 0.055 $\mu S\ cm^{-1}$.

2.2. Chitosan Monolayer Adsorption. To find the appropriate experimental conditions for the first, precursor, layer of chitosan adsorption onto Si substrates, we used three different types of chitosan: low-molecular-weight chitosan (50−190 kDa, LM_w CS), medium-molecular-weight chitosan (190−310 kDa, MM_w CS), and high-molecular-weight chitosan (310−375 kDa, HM_w CS). All CS samples were obtained from Sigma-Aldrich and used as received. The degree of deacetylation (DD) of each chitosan sample was determined by conductometric titration with HCl, as described in the work of Pérez-Álvarez et al. (representative titration of LM_w CS is shown in Figure S1).[45] The values of DD were ∼75% for LM_w CS and ∼92% for MM_w CS (both in line with the DD values reported by the manufacturer), while for HM_w CS, due to issues with solubility, DD was difficult to be properly ascertained, but according to the Certificate of Analysis provided by the manufacturer, it is ≥75%. CS solutions were prepared by dissolving the required amount of CS in 1% w/w CH_3COOH (Chem-Lab). Multiple concentrations of CS of each type were prepared for solubility experiments, and selected concentrations were used for CS monolayer preparation on Si wafer, with adsorption times of 15 min and 24 h.

2.3. Polyelectrolyte Multilayer Formation. Polyelectrolytes used for multilayer preparation were low-molecular-weight chitosan and carboxymethyl cellulose sodium salt (medium viscosity, Sigma-Aldrich). Both were used as received from the supplier. PEI (linear, M_w = 10 kDa) was obtained from Sigma-Aldrich. Multiple sets of multilayers were prepared:

I. Multilayers without the precursor layer;
II. Multilayers with PEI as the precursor layer;
III. Multilayers with CS as the precursor layer.

To further study multilayer formation under these conditions, the influence of the addition of NaCl was also studied for every set of multilayers. NaCl was obtained from Sigma Aldrich (99.9% purity) and used as is. The concentrations used for multilayer buildup were 1 g dm^{-3} for CS and CMC. The pH of 1 g dm^{-3} CS solution in 1% w/w CH_3COOH was 3, while addition of HCl (Merck) was required to adjust the pH of CMC solution to 3. A 0.01 mol dm^{-3} solution of PEI and a 15 g dm^{-3} low-molecular-weight CS solution, as this concentration was determined to be the most optimal (see Section 3), were used for precursor layer deposition. The pH values of these solutions were 3 (adjusted with HCl) and 4.2, respectively. All pH measurements and adjustments were done using a pH meter (826 pH mobile, Metrohm) equipped with a combined glass microelectrode (6.0234.100, Metrohm), precalibrated with standard buffers (Fluka) of pH 3.0, 7.0, and 9.0.

PEMs were prepared using a conventional layer-by-layer method.[7] The first deposited layer was either CS or PEI; then, the rest of the film was composed by alternating the deposition of CMC and CS up to 10 layers, with CMC being the terminating layer. Each polyelectrolyte layer was deposited for

https://doi.org/10.1021/acsomega.3c02281
ACS Omega 2023, 8, 20031−20041

10 min. After each deposited layer, the wafer was rinsed three times in water, first for 2 min and twice for 1 min and then dried with a stream of argon gas. This process was repeated until the planned number of layers (10) was deposited onto the substrate. The notation of the films $(CS/CMC)_n$ represents their composition, and n is the number of layers.

2.4. Ellipsometry Measurements. Thickness measurements of both monolayers and PEMs were done on an L116B-USB ellipsometer from Gaertner Scientific Corporation. The measurements were performed under ambient conditions (25−55% relative humidity and 25 °C) using red He−Ne laser light with a wavelength of 632.8 nm at a fixed incident angle of 70°. This angle was chosen due to its closeness to the Brewster angle of the silicon/air interface of 75.5°.[46] For the collection and processing of data, Gaertner Ellipsometric Measurement Program (Version 8.071) package was used. The software used a three-box model with air as a continuum (n = 1.00),[47] multilayer as a one-phase system with a refractive index of 1.457[48] that is independent of the film composition and thickness, and Si wafer as a substrate was assumed. The Si/SiO_x substrate was treated as a one-phase system. Before the adsorption of any polyelectrolyte on the surface, the refractive index of each used substrate was determined separately by measuring different positions on each substrate. Afterward, following the adsorption of each layer of the PEM, its thickness was determined at 10 different locations on each sample and presented as an average (with the standard deviation) of measurements.

2.5. Atomic Force Microscopy Measurements. The surface properties (topography, surface roughness, and film thickness) of all prepared samples were determined by atomic force microscopy using a Multimode 8E AFM apparatus from Bruker. All measurements were done in tapping mode using NCHV-A probes (Bruker). The probes were 117 μm in length and 33 μm in width with a resonance frequency of approximately 320 kHz and a nominal spring constant of 40 N/m. The tip height was 10−15 μm having a nominal radius of curvature of 8 nm. All the AFM measurements were carried out in ambient air conditions.

All AFM scans were done on a 5 × 5 μm^2 area with a scanning rate of 1 Hz and a picture resolution of 512 × 512 $pixels^2$. The data were processed in NanoScope Scan 9.7, and AFM images were corrected for tilt and bow using a second order flattening and were analyzed in NanoScope Analysis 2.0 software to determine the local root-mean-square (RMS) roughness of LbL films. AFM roughness parameters and appropriate standard deviations reported here were calculated from all the measurements, which included five local areas on each sample surface. Multilayer thicknesses of the films were determined by gently removing a portion of the film from the substrate surface with a sharp tweezer (model: EM-Tec 3C.AM, micro to nano) and analyzing the cross sections of the scanned image. Then, the measurements were made by scanning the AFM tip across the step edge boundary in a soft tapping mode. Finally, the total film thickness was calculated using the sophisticated terrace feature in Gwyddion 2.54 software after an ordinary first-order flattening routine in NanoScope Analysis 2.0 program. Gwyddion 2.54 software shows the results in the form of an average film thickness and its standard deviation, as reported in the manuscript.

3. RESULTS

As mentioned in Introduction, this study consists of two parts. In the first part, we investigated the preparation of a suitable first chitosan layer to act as its own precursor layer for the multilayer buildup done in the second stage of the study.

3.1. Determination of Optimal Precursor Chitosan Layer for Multilayer Buildup. The first step was to examine the solubility of different chitosan samples in acetic acid. The results of these experiments are shown in Table S1. The results confirmed that LM_w CS has the highest solubility, while HM_w CS could not be fully dissolved in these experimental conditions. Based on the results, we selected chitosan solutions marked with * in Table S1 as the possible starting solutions for the preparation of a precursor layer. It should be noted that for the 4 g dm^{-3} HM_w CS solution, the leftover undissolved chitosan was decanted, so that a clear solution was obtained. The results of the next set of experiments, adsorption of a single layer of CS on a silica surface, and the respective film thicknesses, d, determined by ellipsometry, are presented in Figure 1.

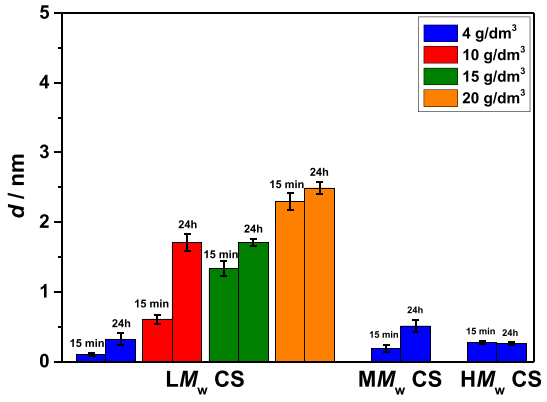

Figure 1. Influence of deposition time, polyelectrolyte concentration, and chitosan molecular weight on the monolayer thickness determined by ellipsometry.

Multiple conclusions can be drawn from the results presented in Figure 1. First, comparing 4 g dm^{-3} chitosan solutions of all examined molecular weights, the results show that molecular weight does not significantly influence the film thickness. The thickness of all these films was <1 nm, irrelevant of the deposition time. Second, as LM_w CS is the most soluble one, we prepared solutions of higher concentrations of it, and the increase of concentration proved to be the determining factor that influences the thickness of the prepared films. This increase was to about 0.5 nm for 10 g dm^{-3} solution and to 1.5−2 nm for higher concentrations. Unfortunately, as the concentration of LM_w CS increased, removing excess polyelectrolytes from the surface of the substrate and subsequent drying of the adsorbed film got increasingly difficult. This culminated with a 20 g dm^{-3} solution, where removing weakly bound polyelectrolytes proved to be difficult due to the solution viscosity. Hence, the results of 20 g dm^{-3} solution could not be adequately reproduced, and this concentration was deemed unfit as a precursor candidate. Finally, the increase in deposition time leads to thicker films. The difference in the thickness of monolayers deposited for 15 min and 24 h is more pronounced for lower concentrations of chitosan compared to higher concentrations. This can be

https://doi.org/10.1021/acsomega.3c02281
ACS Omega 2023, 8, 20031−20041

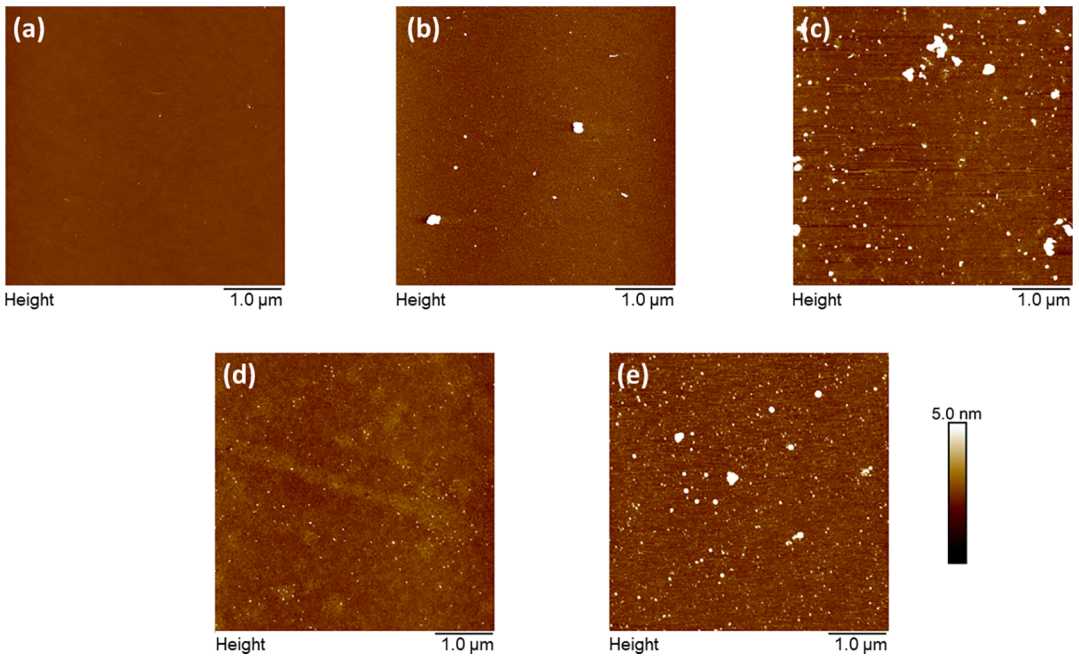

Figure 2. AFM images of (a) Si wafer surface, and Si surfaces with the prepared LM_w chitosan layer adsorbed at different conditions: (b) 4 g dm^{-3} solution for 15 min; (c) 4 g dm^{-3} solution for 24 h; (d) 10 g dm^{-3} solution for 15 min; and (e) 15 g dm^{-3} solution for 15 min.

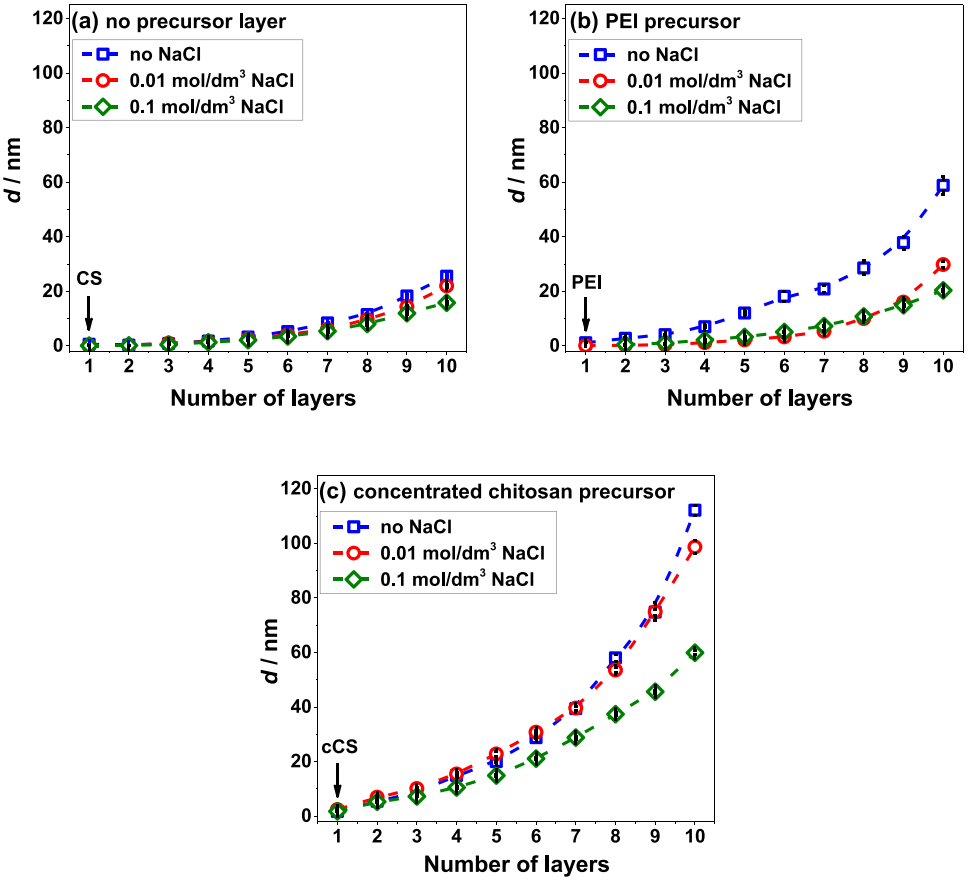

Figure 3. PEM film thickness of CS/CMC multilayers as a function of the number of deposited polyelectrolyte layers on a Si substrate: (a) films without the precursor layer; (b) films with PEI; and (c) films with chitosan deposited from a concentrated solution (cCS) as the precursor layer. Dashed lines were added as guides to the eye.

attributed to faster adsorption kinetics of the more concentrated CS solution to Si surfaces. Afterward, selected chitosan layers were investigated, with the focus being on the films deposited for 15 min, as the adsorption time of 24 h would be impractical for any potential application of these films. AFM was used to ascertain the differences in film

https://doi.org/10.1021/acsomega.3c02281
ACS Omega 2023, 8, 20031−20041

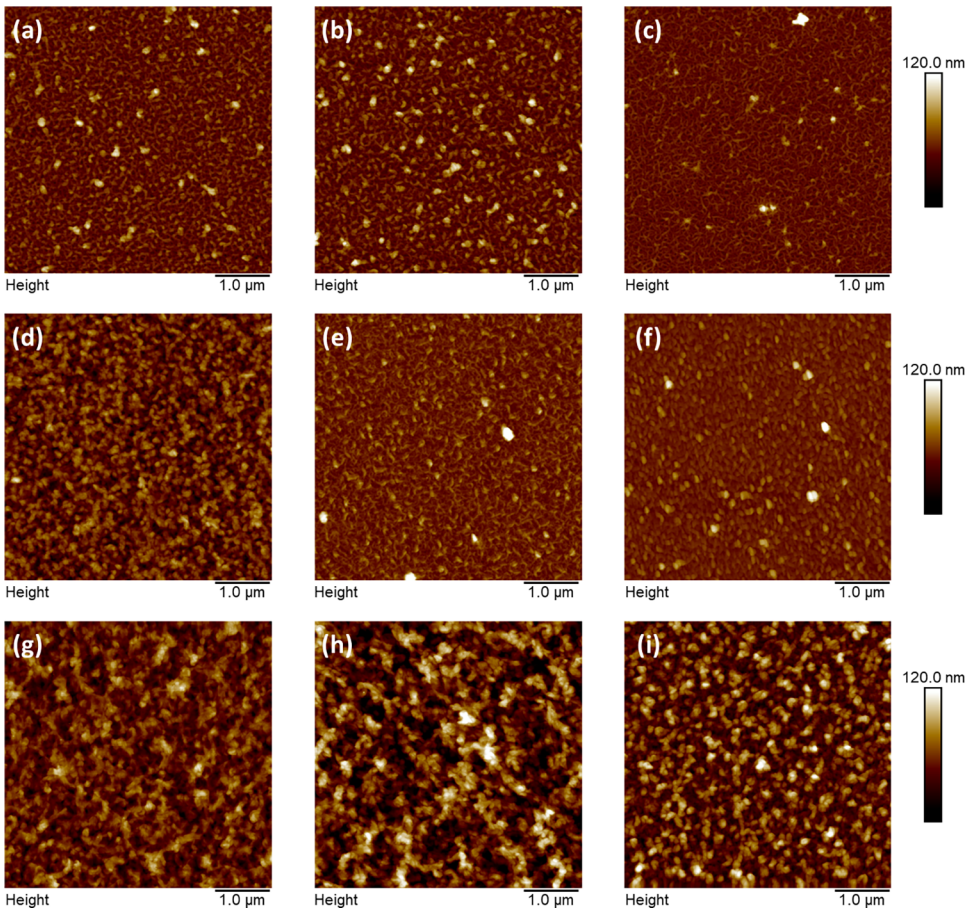

Figure 4. AFM images of the prepared 10-layer CS/CMC PEMs: (a–c) without the precursor layer; (d–f) with PEI as the precursor layer; (g–i) with concentrated CS as the precursor layer. The first column of images shows films without added NaCl; the second column shows nanofilms with 0.01 mol dm^{-3} NaCl added; and the third with 0.1 mol dm^{-3} NaCl added.

morphology and to get the idea of the surface coverage by the film. Representative AFM images of the investigated films can be seen in Figure 2.

Figure 2a shows the reference silica substrate surface, and it is flat without impurities. Figure 2b shows the Si surface, with chitosan adsorbed for 15 min from 4 g dm^{-3} solution. Although most of this sample's surface is similar to the surface shown in Figure 2a, nanosized islets of various sizes can be seen scattered throughout the area. In comparison to Figure 2c, which shows chitosan adsorbed from the same solution but for 24 h, the surface morphology looks slightly different, and the islets are more numerous and larger. Continuing to the film deposited from 10 g dm^{-3} solution for 15 min, Figure 2d, its surface looks like the surface of the sample in Figure 2c, with the notable difference of the islets being very small but scattered throughout the whole surface area. Increasing the chitosan concentration to 15 g dm^{-3}, Figure 2e, the morphology is reminiscent of the sample pictured in Figure 2c, as there is a notable difference in the morphology of the surface compared to the untreated Si wafer with numerous islets and structures throughout the surface. From all these results, it can be inferred that the surface coverage of the first layer of chitosan is more dependent on concentration than adsorption time in these experimental conditions.

3.2. Characterization of CS/CMC Nanofilms. *3.2.1. Chitosan/Carboxymethyl Cellulose Multilayer Film Growth.* In the next part of our study, we prepared three types of CS/CMC multilayers: PEMs without any precursor layer, PEMs with PEI as a precursor layer, and PEMs with the chitosan monolayer adsorbed from the 15 g dm^{-3} solution as a precursor layer. In addition, we investigated the influence of the addition of NaCl to the deposition solutions on the film growth and its properties. Figure 3 shows the film growth of all prepared nanofilms monitored by ellipsometry.

The first commonality between all films prepared with or without a precursor layer is that all of them follow the exponential growth regime. In addition, the increase in salt concentration leads to the formation of thinner films. Delving further into each set of the prepared 10-layer films, those prepared without any precursor layer, Figure 3a, are the thinnest, with the thickest of them being 25.5 ± 0.5 nm thick. The addition of NaCl lowers the thickness to 22.0 ± 0.5 and 15.8 ± 0.6 nm for the films with 0.01 and 0.1 mol dm^{-3} NaCl, respectively. Following this, Figure 3b shows the film growth of the multilayers, with PEI as the precursor layer, and the thickness of the film without NaCl is more than double the thickness of the film prepared without a precursor layer, 58.8 ± 3.5 nm. Accordingly, the values of thickness of the films with added NaCl are also higher compared to the films in Figure 3a but by a much smaller margin, 29.8 ± 1.1 and 20.4 ± 0.3 nm for 0.01 and 0.1 mol dm^{-3} NaCl, respectively. Interestingly, a drastic increase of thickness is only observed for the film without any addition of NaCl. Finally, in Figure 3c, the growth of multilayers with CS as the precursor layer is shown. In this

https://doi.org/10.1021/acsomega.3c02281
ACS Omega 2023, 8, 20031–20041

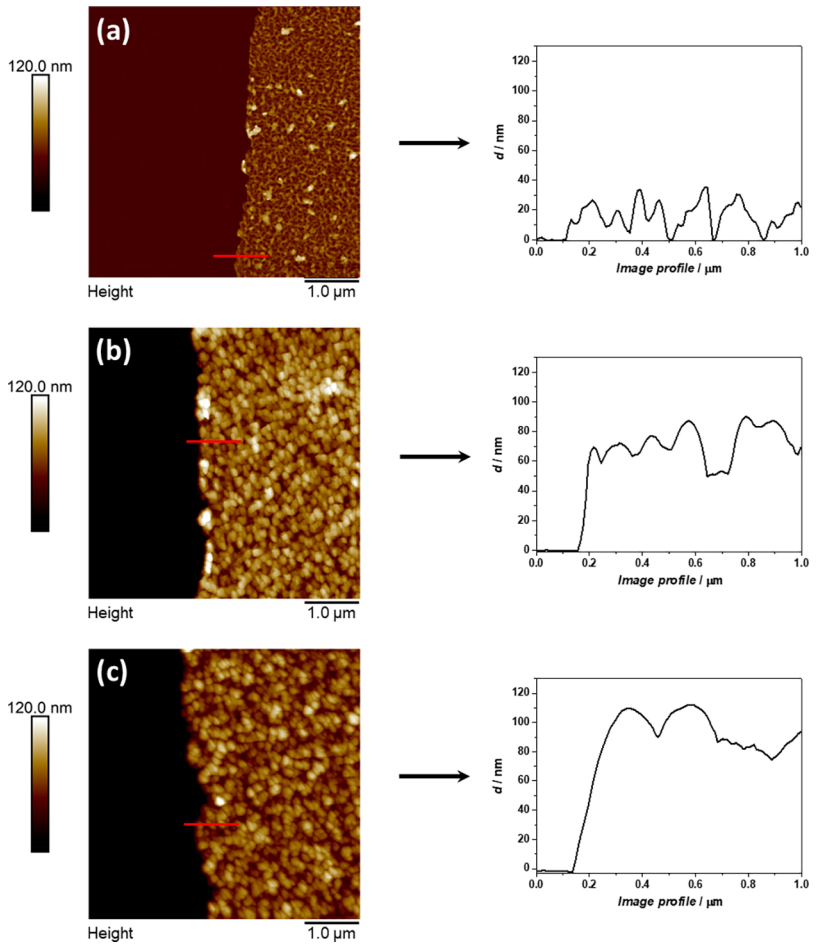

Figure 5. Cross sections and the corresponding height profiles (red lines on the AFM images) of films prepared (a) without the precursor layer, (b) with PEI, and (c) with chitosan deposited out of the concentrated solution as a precursor layer. Multilayers were prepared without the background salt.

case, the multilayer prepared without NaCl has almost double the thickness of the one prepared with PEI, 112.2 ± 1.8 nm, meaning this is a quadruple increase compared to the film without any precursor layer. Next, the film prepared in the presence of 0.01 mol dm^{-3} NaCl also shows a large increase in thickness, 98.7 ± 2.2 nm, compared to previous films with the same NaCl concentration. Lastly, the film with the largest concentration of NaCl is again the thinnest, 59.9 ± 0.8 nm, by a substantial amount, but, compared to other films prepared with these experimental parameters, shows a significant increase due to the CS precursor layer.

3.2.2. Chitosan/Carboxymethyl Cellulose Multilayer Surface Imaging. To further characterize the obtained multilayers, different microscopic methods were used. Figure S2 shows the representative images of the nanofilms taken by a digital optical microscope camera (Nikon 10x-A). First, films prepared without a precursor layer have no distinguishing markings on the surface. Second, films prepared with PEI but without the addition of NaCl showed a notable blue coloration. On the other hand, films with both PEI and NaCl lack the blue hue, but the features on the surface indicate the presence of a film on the Si surface. Finally, all films prepared with CS as the precursor layer show pronounced blue coloration of the surface compared to the bluish hue. Notably, the film prepared with CS as the precursor layer and without any NaCl, Figure S2g, has a distinct blue color which covers the entire surface of the substrate. This coloration diminishes with the addition of NaCl but is still notable. The most similar colored films are the ones shown in Figure S2d,i. We believe this coloration is linked to the film thickness and to the amount and size of the pores on the surface of the film itself.

Going further, all films were examined by AFM, and representative images can be seen in Figure 4. The first row of images, Figure 4a−c, shows the films prepared without the precursor layer. The morphology of these films consists of small islets which are interconnected by wormlike structures. In the second row of images, Figure 4d−f, a pattern is formed. While the morphology of the film prepared with PEI and without NaCl, Figure 4d, consists connected grain-like structures, the films prepared in the presence of NaCl, Figure 4e,f, are morphologically similar to the films without PEI, Figure 4a−c. This morphological similarity can be linked to the similarity in the thickness of these films; they are all 15−30 nm thick compared to the one in Figure 4d which is ∼60 nm thick. In the last row of images, which shows the films with concentrated CS as the precursor layer, Figure 4g−i, the morphology drastically differs compared to all other films. Upon closer inspection, the morphology reminds of the wormlike connecting structures shown in Figure 4a−f but with the structures being thicker and more connected with no noticeable grains on the surface. It should be noted that films prepared without NaCl and with 0.01 mol dm^{-3} NaCl, Figure

https://doi.org/10.1021/acsomega.3c02281
ACS Omega 2023, 8, 20031−20041

4g,h, have a similar morphology. At the same time, the film with CS as the precursor layer with the addition of 0.1 mol dm^{-3} NaCl, Figure 4i, looks like the film prepared with PEI as the precursor layer with no addition of NaCl, Figure 4d. Again, these morphological similarities can be linked to the similarities of thicknesses of these films, the first pair of films being ∼100 nm thick, while the second pair ∼60 nm.

The next step of surface imaging was the determination of the porosity of the films by analyzing the cross sections of the multilayers after removing a part of the film with a sharp tweezer, as described in Section 2. Figure 5 shows the porosity examinations of all films without the added background salt.

From Figure 5, it can be observed that the film without a precursor layer is porous as the height profile shows that the film thickness decreases down to the substrate surface, $d = 0$, Figure 5a. This trend is absent in the height profiles of both films which have a precursor layer present, Figure 5b,c. Additionally, the same analysis of the films with the added background NaCl of both concentrations has shown the same result where the presence of the precursor layer guaranteed full surface coverage by the film (Figures S3−S5). Finally, we analyzed all AFM images with Nanoscope and Gwyddion software to determine the surface roughness and thickness of all examined nanofilms.

3.2.3. Determination of Surface Roughness and Film Thickness by AFM. The results of the local RMS surface roughness, R_q, and thickness, d, analyses can be found in Figures 6 and 7, respectively.

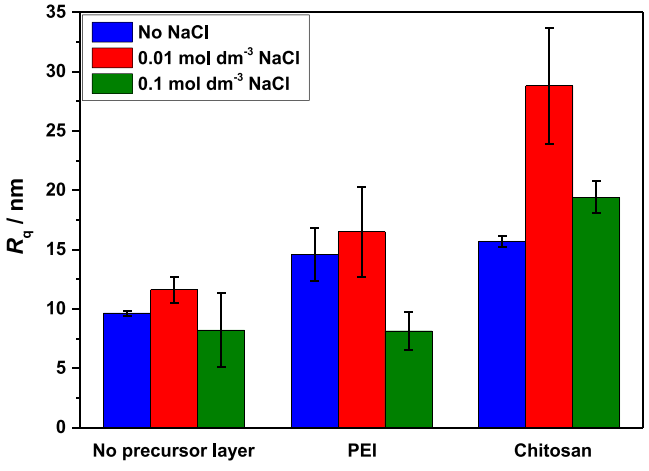

Figure 6. Surface roughness, R_q, of CS/CMC films prepared with and without the precursor layers and supporting salt of different concentrations.

From the first look at Figure 6, one can see an increase in film roughness with the addition of precursor layers. Additionally, at the first glance, the effect of the background NaCl is the same for all three sets of films, but slight variations must be considered. First, in the case of films without the precursor layer, the change in R_q with the addition of NaCl is within experimental error, and the value of R_q is about 9 nm. From this, we can infer that in this case, NaCl has a negligible influence on surface roughness. In the second set of films, with PEI, the films without the added NaCl and with 0.01 mol dm^{-3} of NaCl have similar roughness (∼15 nm), but the addition of 0.1 mol dm^{-3} NaCl leads to a drop of roughness to about 8 nm. Finally, the third set of films, with CS as the precursor, has

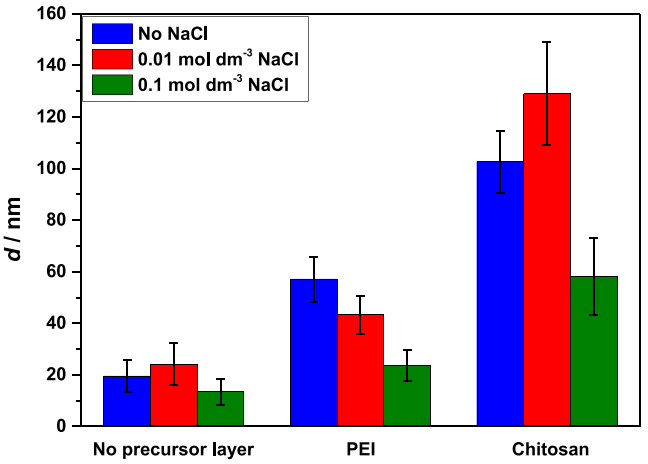

Figure 7. Film thickness of the prepared CS/CMC multilayers (10 layers) determined by AFM.

the highest values of roughness, irrelevant of NaCl concentration. Furthermore, we were surprised by the result of the CS precursor film with 0.01 mol dm^{-3} NaCl which had double the roughness of its variant without NaCl, ∼29 nm compared to ∼16 nm. Further addition of NaCl only led to a slight increase of R_q value to ∼20 nm compared to the film without NaCl.

Lastly, to determine the thickness of the films by AFM, we removed a part of the film from the surface of the substrate with sharp tweezers, as mentioned in Section 2 and shown in Figure 5. Figure 7 summarizes our findings.

The results presented in Figure 7 confirm the ellipsometry results, Figure 3, where the presence of a precursor layer increases the film thickness. In terms of ionic strength effect, generally, the thickness decreases with the increase in salt concentration, at least in the examined salt range and for the examined pair of polyelectrolytes. However, we observed slight discrepancies between the thickness results obtained by ellipsometry, Figure 3, and AFM, Figure 7, that can be explained by the porosity and roughness of the films. Unfortunately, ellipsometry optical models used for the calculation of film thickness do not consider the porosity and roughness of the films. In the cases of the films without the precursor layer and with concentrated CS as the precursor layer, the thickest films are the ones with the added 0.01 mol dm^{-3} of NaCl compared to ellipsometry results where the thickest film was always the one without NaCl.

In addition, when one looks at the trends of surface roughness, Figure 6, and compares them to the trends of film thickness determined by AFM, Figure 7, similarities can be observed where the middle values are the ones without added NaCl, which are then increased slightly in the presence of 0.01 mol dm^{-3} NaCl, followed by a drop to lower values at a higher salt concentration. However, this decrease in value is larger for the films with CS as the precursor, 55%, compared to 44−45% for films without the precursor layer or with PEI.

Going further, considering the experimental error, for the multilayers without the precursor layer, one can say that the values of both roughness and thickness determined by AFM are more or less of constant value, so in this case, the addition of NaCl has minimal or no effect on these parameters. This trend continues for the multilayers with PEI as the precursor layer but with a significant drop of values in both thickness and roughness for the film with 0.1 mol dm^{-3} NaCl. Finally, for the

https://doi.org/10.1021/acsomega.3c02281
ACS Omega 2023, 8, 20031−20041

set of films with CS as the precursor, the trend in thickness follows the trend of the films with PEI, where the initial addition of the background salt has no effect on the multilayer thickness, which is followed by a large drop for 0.1 mol dm^{-3} of NaCl. Meanwhile, the roughness trend differs in the fact that the R_q value of the multilayer with 0.01 mol dm^{-3} NaCl is much higher than the ones without NaCl or with 0.1 mol dm^{-3} NaCl added.

4. DISCUSSION

To summarize, our results confirmed that the adsorption of the first layer chitosan from a solution with increased concentration can produce PEMs with more pronounced properties compared to the properties of films without the precursor layer or with, the current mainstream, PEI. In terms of potential application, this means, first and foremost, one can create a fully biocompatible, highly tunable coating, especially for the protection of natural products like fruits. This biocompatibility is of crucial value due to the already mentioned toxicity of PEI which is reported in the literature.[20−23] Second, by creating thicker films compared to PEI, one can argue that less material is needed to fully coat a fruit's surface, which equates the economic savings. To explain these differences between PEI and CS as precursor layers, one needs to examine the nature and structure of the polyelectrolytes used in this study.

To start, all polyelectrolytes used in this study are weak polyelectrolytes, so the pH of their solutions used for the buildup needs to be addressed. For this, using the Henderson−Hasselbalch equation, we calculated the ratio of the charged form of each polyelectrolyte, knowing their pK_a values: ∼6.2 for chitosan, ∼7 for poly(ethyleneimine), and ∼4.5 for carboxymethyl cellulose.[49−51] Using the pH value at which the experiments were performed (pH = 3.0) as the reference for the calculation, we have found, as expected, that most of CS and PEI carry positive charge on their amine groups. Conversely, at the examined pH value, the carboxyl groups of CMC are in their protonated form. From this info, we can conclude that the forces driving the multilayer buildup of this system cannot be purely electrostatic due to the lack of $-COO^-$ charge on CMC to bind to positively charged $-NH_3^+$ groups of PEI or CS. Hence, other intermolecular forces, such as hydrogen bonding, must be involved. This is in agreement with the results of a recent paper by Tirrell and co-workers[52] who have demonstrated that poly(allylamine hydrochloride) and poly(acrylic acid) polyelectrolyte complexes can establish hydrogen bonding at low pH values. In some other polyelectrolyte systems, hydrogen bonding has also been reported as the driving force for the multilayer buildup.[53−56] For instance, Markarian et al.[16] have investigated the difference in polyelectrolyte multilayer buildup where different polynucleotides gave rise to different types of binding between polyelectrolyte molecules. Similarly, as CS and CMC are polysaccharides with plentiful hydrogen donor and acceptor groups, multilayer buildup assisted by hydrogen bonding is possible and has already been detected in some other materials containing CS and CMC.[57−59]

To further explain the difference on how hydrogen bonding influences these films, we must compare ellipsometry and AFM measurements. From Figure 3, we can see that the buildup of all films prepared in this study is exponential but differs slightly depending on the type of the precursor layer. In the first set of multilayers, the ones without the precursor layer, Figure 3a, there is no noticeable difference between the growth regimes of the films in the presence of different NaCl concentrations. This is also confirmed via surface morphology and the trends of surface roughness and film thickness, as determined by AFM, Figures 4, 6, and 7. Continuing to the films with PEI as the precursor, the exponential growth regime of the multilayer without the added salt is more pronounced than the growth regimes of the multilayers with the added salt which are the same up to and including the ninth layer, Figure 3b. This result is also confirmed by the AFM measurements and thickness and roughness trends. In the last set of multilayers, with CS as the precursor, Figure 3c, the growth regimes are inverted compared to the growth regimes of the films with PEI. In this case, the films without NaCl and with lower NaCl concentration are roughly the same up to and including the 9th layer, while the multilayer with 0.1 mol dm^{-3} NaCl grows more slowly. Such a conclusion is also backed by AFM results where multilayers without NaCl and with 0.01 mol dm^{-3} NaCl are morphologically almost identical, Figure 4g,h, while the multilayer with 0.1 mol dm^{-3} NaCl is more like the one with PEI as the precursor obtained without NaCl, Figure 4d,i. Additionally, with regard to Figure 3c, we need to digress and add a minor comment on the multilayers without the precursor layer, Figure 3a. Zooming in on the Y scale of Figure 3a, the growth regimes of the multilayers are reminiscent to the ones present in Figure 3c but not as pronounced. This is most likely due to the low initial adsorption of chitosan to the substrate surface from the 1 g dm^{-3} solution. Hence, this result further proves that the multilayer buildup in the first few layers is crucial for its growth and final properties.

From these results, one can infer that PEI and CS act differently when used as the first layer. In this study, we used linear PEI which consists of secondary amine groups interlinked by ethylene groups. While an amine group on its own can be a good acceptor and donor of hydrogen bonding, at pH 3, it is protonated, so it loses the ability to accept hydrogen bonds. This diminishes the binding of the next CMC layer as it lacks negative charges to bind to PEI electrostatically, while at the same time it has a lower ability to bind to PEI with hydrogen bonds. On the contrary, using CS adsorbed from a solution with increased concentration as a precursor adds the ability of hydrogen bonding to occur from the start of the multilayer buildup, which, in the end, results in more pronounced film growth and thicker films.

Finally, a comment on the effect of the background salt is needed. One of the unexpected results of this study was that the increase in ionic strength does not necessarily produce films with higher thickness, as is typically shown for other polyelectrolyte systems.[10,14,15] This is likely because the addition of NaCl to such systems hinders the interactions between polyelectrolytes due to the charge oversaturation and screening of hydrogen-bond sites. This inability to create hydrogen bonds and the lack of electrostatic interactions results in thinner films. From our results, we can assume that the case of the lower concentration of NaCl (0.01 mol dm^{-3}) does not provide the critical concentration of ions to produce the charge and hydrogen-bond site screening effect. Raising the concentration of NaCl to 0.1 mol dm^{-3}, the growth regimes of all prepared films slow down, which is prompted by the increase of the number of ions in the solution enough to hinder the binding of the polyelectrolytes.

https://doi.org/10.1021/acsomega.3c02281
ACS Omega 2023, 8, 20031−20041

5. CONCLUSIONS

The main idea of this study was to replicate the effects of PEI, a synthetic polymer, as a precursor layer on the buildup and properties of CS/CMC multilayers on silica substrates with a biocompatible substitute, at the same time tuning the properties of the prepared PEMs with the addition of NaCl. In the first stage of this study, we focused on the fabrication of the satisfactory precursor layer out of CS with different molecular weights. We have found that CS of lower molecular weights can be dissolved in 1% acetic acid in high quantities (up to 20 g dm^{-3}), so this made it a prime candidate for the preparation of an adequate precursor layer. In the second part of this study, we prepared CS/CMC nanofilms with different precursor layers, PEI, and CS monolayer using the layer-by-layer method and compared the properties of the prepared films with each other and with the properties of those without any precursor layer. Using ellipsometry and AFM, our results have shown that using a precursor layer leads to a twofold increase of thickness in the case of PEI, and a fourfold in the case of CS, compared to the films prepared without any precursor layer present. AFM measurements have shown that the addition of a precursor layer also increases the surface roughness of the films, which is more pronounced in the case of CS as the precursor. Also, the addition of precursor layers changed the film structure from being porous to compact, which is a highly desirable trait for the potential future application of these materials. Conversely, the addition of background NaCl to the deposition solutions leads to a different effect depending on its concentration. At a low concentration, its effect on film thickness is low or nonexistent but can lead to an increased surface roughness, while a high concentration produces an opposite effect, lowering both thickness and roughness. This effect can be explained by the fact that this combination of polyelectrolytes forms nanofilms stabilized not only by electrostatic interactions but also by hydrogen bonding. The decrease of film thickness can be attributed to the competing effect of adsorbed polyelectrolytes and NaCl with the polyelectrolytes in the solution to form hydrogen bonds during multilayer buildup.

Our results confirmed that using a more concentrated solution of chitosan for the buildup of the first layers of a nanofilm, as a precursor layer, is a valid natural and biocompatible alternative to the currently widespread use of PEI. Such a precursor layer is not only viable but also modifies the surface properties of the prepared nanofilms in different ways compared to PEI. Moreover, if needed, these properties can be fine-tuned by the presence of NaCl in the deposition solutions, creating fully biocompatible nanocoatings. However, one issue which arises with using concentrated CS as a precursor layer compared to PEI is the higher surface roughness which could lead to a higher adsorption of unwanted bacteria to the film and its degradation.[60] In the next step of our studies of these materials, we see the potential of the possible post-treatment of the prepared PEMs with salt (salt annealing)[61] as an additional method for the fine-tuning of their properties. To sum up, our results provide a framework for obtaining tunable, completely biocompatible chitosan–carboxymethyl cellulose nanofilm coatings with optimized physicochemical properties for applications in food science and nanomedicine.

ASSOCIATED CONTENT

Supporting Information

The Supporting Information is available free of charge at https://pubs.acs.org/doi/10.1021/acsomega.3c02281.

Conductometric titration curve used for the determination of the degree of deacetylation for low-molecular-weight chitosan; results of solubility experiments of different molecular weights of chitosan; digital optical microscope images of the prepared nanofilms; and cross sections and the corresponding height profiles of all films prepared with the addition of NaCl (PDF)

AUTHOR INFORMATION

Corresponding Authors

Juraj Nikolić − *Division of Physical Chemistry, Department of Chemistry, Faculty of Science, University of Zagreb, 10000 Zagreb, Croatia;* orcid.org/0000-0002-0548-4185; Email: jnikolic@chem.pmf.hr

Davor Kovačević − *Division of Physical Chemistry, Department of Chemistry, Faculty of Science, University of Zagreb, 10000 Zagreb, Croatia;* orcid.org/0000-0001-6446-3459; Email: davor.kovacevic@chem.pmf.hr

Authors

Ana Ivančić − *Division of Physical Chemistry, Department of Chemistry, Faculty of Science, University of Zagreb, 10000 Zagreb, Croatia*

Tin Klačić − *Division of Physical Chemistry, Department of Chemistry, Faculty of Science, University of Zagreb, 10000 Zagreb, Croatia;* orcid.org/0000-0003-2506-8688

Complete contact information is available at: https://pubs.acs.org/10.1021/acsomega.3c02281

Author Contributions

The manuscript was written through contributions of all authors. All authors have given approval to the final version of the manuscript. All authors contributed equally.

Funding

The authors thank the Croatian Science Foundation for financing this research under project IPS-2020-01-6126.

Notes

The authors declare no competing financial interest.

ACKNOWLEDGMENTS

The authors thank the European Regional Development Fund−−infrastructural project CIuK (KK.01.1.1.02.0016) for support. J.N. thanks V. Nemec for fruitful discussions.

REFERENCES

(1) El-Saber Batiha, G.; Hussein, D. E.; Algammal, A. M.; George, T. T.; Jeandet, P.; Al-Snafi, A. E.; Tiwari, A.; Pagnossa, J. P.; Lima, C. M.; Thorat, N. D.; Zahoor, M.; El-Esawi, M.; Dey, A.; Alghamdi, S.; Hetta, H. F.; Cruz-Martins, N. Application of Natural Antimicrobials in Food Preservation: Recent Views. *Food Control* **2021**, *126*, No. 108066.

(2) Zhang, X.; Ismail, B. B.; Cheng, H.; Jin, T. Z.; Qian, M.; Arabi, S. A.; Liu, D.; Guo, M. Emerging Chitosan-Essential Oil Films and Coatings for Food Preservation - A Review of Advances and Applications. *Carbohydr. Polym.* **2021**, *273*, No. 118616.

(3) Ju, J.; Xie, Y.; Guo, Y.; Cheng, Y.; Qian, H.; Yao, W. Application of Edible Coating with Essential Oil in Food Preservation. *Crit. Rev. Food Sci. Nutr.* **2019**, *59*, 2467−2480.

(4) Zambrano-Zaragoza, M. L.; González-Reza, R.; Mendoza-Muñoz, N.; Miranda-Linares, V.; Bernal-Couoh, T. F.; Mendoza-Elvira, S.; Quintanar-Guerrero, D. Nanosystems in Edible Coatings: A Novel Strategy for Food Preservation. *Int. J. Mol. Sci.* **2018**, *19*, 705.
(5) Chen, W.; Ma, S.; Wang, Q.; McClements, D. J.; Liu, X.; Ngai, T.; Liu, F. Fortification of Edible Films with Bioactive Agents: A Review of Their Formation, Properties, and Application in Food Preservation. *Crit. Rev. Food Sci. Nutr.* **2022**, *62*, 5029−5055.
(6) Lichter, J. A.; Van Vliet, K. J.; Rubner, M. F. Design of Antibacterial Surfaces and Interfaces: Polyelectrolyte Multilayers as a Multifunctional Platform. *Macromolecules* **2009**, *42*, 8573−8586.
(7) Decher, G.; Hong, J. D.; Schmitt, J. Buildup of Ultrathin Multilayer Films by a Self-Assembly Process: III. Consecutively Alternating Adsorption of Anionic and Cationic Polyelectrolytes on Charged Surfaces. *Thin Solid Films* **1992**, *210-211*, 831−835.
(8) Criado-Gonzalez, M.; Mijangos, C.; Hernández, R. Polyelectrolyte Multilayer Films Based on Natural Polymers: From Fundamentals to Bio-Applications. *Polymers* **2021**, *13*, 2254.
(9) Nascimento, V.; França, C.; Hernández-Montelongo, J.; Machado, D.; Lancellotti, M.; Cotta, M.; Landers, R.; Beppu, M. Influence of PH and Ionic Strength on the Antibacterial Effect of Hyaluronic Acid/Chitosan Films Assembled Layer-by-Layer. *Eur. Polym. J.* **2018**, *109*, 198−205.
(10) Lundin, M.; Solaqa, F.; Thormann, E.; Macakova, L.; Blomberg, E. Layer-by-Layer Assemblies of Chitosan and Heparin: Effect of Solution Ionic Strength and PH. *Langmuir* **2011**, *27*, 7537−7548.
(11) Mesić, M.; Klačić, T.; Abram, A.; Bohinc, K.; Kovačević, D. Role of Substrate Type in the Process of Polyelectrolyte Multilayer Formation. *Polymers* **2022**, *14*, 2566.
(12) Jukić, J.; Korade, K.; Milisav, A. M.; Marion, I. D.; Kovačević, D. Ion-Specific and Solvent Effects on PDADMA−PSS Complexation and Multilayer Formation. *Colloids Interfaces* **2021**, *5*, 38.
(13) Klačić, T.; Bohinc, K.; Kovačević, D. Suppressing the Hofmeister Anion Effect by Thermal Annealing of Thin-Film Multilayers Made of Weak Polyelectrolytes. *Macromolecules* **2022**, *55*, 9571−9582.
(14) Steitz, R.; Jaeger, W.; Klitzing, R. V. Influence of Charge Density and Ionic Strength on the Multilayer Formation of Strong Polyelectrolytes. *Langmuir* **2001**, *17*, 4471−4474.
(15) Tang, K.; Besseling, N. A. M. Formation of Polyelectrolyte Multilayers: Ionic Strengths and Growth Regimes. *Soft Matter* **2016**, *12*, 1032−1040.
(16) Markarian, M. Z.; Mousallem, M. D.; Jomaa, H. W.; Schlenoff, J. B. Hydrogen Bonding versus Ion Pairing in Polyelectrolyte Multilayers with Homopolynucleotides. *Biomacromolecules* **2007**, *8*, 59−64.
(17) Kolasinska, M.; Krastev, R.; Gutberlet, T.; Warszynski, P. Layer-by-Layer Deposition of Polyelectrolytes. Dipping versus Spraying. *Langmuir* **2009**, *25*, 1224−1232.
(18) Trybała, A.; Szyk-Warszyńska, L.; Warszyński, P. The Effect of Anchoring PEI Layer on the Build-up of Polyelectrolyte Multilayer Films at Homogeneous and Heterogeneous Surfaces. *Colloids Surf., A* **2009**, *343*, 127−132.
(19) Lyu, X.; Peterson, A. M. The Princess and the Pea Effect: Influence of the First Layer on Polyelectrolyte Multilayer Assembly and Properties. *J. Colloid Interface Sci.* **2017**, *502*, 165−171.
(20) Brunot, C.; Ponsonnet, L.; Lagneau, C.; Farge, P.; Picart, C.; Grosgogeat, B. Cytotoxicity of Polyethyleneimine (PEI), Precursor Base Layer of Polyelectrolyte Multilayer Films. *Biomaterials* **2007**, *28*, 632−640.
(21) Gibney, K. A.; Sovadinova, I.; Lopez, A. I.; Urban, M.; Ridgway, Z.; Caputo, G. A.; Kuroda, K. Poly(Ethylene Imine)s as Antimicrobial Agents with Selective Activity. *Macromol. Biosci.* **2012**, *12*, 1279−1289.
(22) Omidi, Y.; Kafil, V. Cytotoxic Impacts of Linear and Branched Polyethylenimine Nanostructures in A431 Cells. *BioImpacts* **2011**, *1*, 23−30.
(23) Lv, H.; Zhang, S.; Wang, B.; Cui, S.; Yan, J. Toxicity of Cationic Lipids and Cationic Polymers in Gene Delivery. *J. Controlled Release* **2006**, *114*, 100−109.
(24) Haghighi, H.; Licciardello, F.; Fava, P.; Siesler, H. W.; Pulvirenti, A. Recent Advances on Chitosan-Based Films for Sustainable Food Packaging Applications. *Food Packag. Shelf Life* **2020**, *26*, No. 100551.
(25) Han, C.; Zhao, Y.; Leonard, S. W.; Traber, M. G. Edible Coatings to Improve Storability and Enhance Nutritional Value of Fresh and Frozen Strawberries (Fragaria x Ananassa) and Raspberries (Rubus Ideaus). *Postharvest Biol. Technol.* **2004**, *33*, 67−78.
(26) Coma, V.; Deschamps, A.; Martial-Gros, A. Bioactive Packaging Materials from Edible Chitosan Polymer - Antimicrobial Activity Assessment on Dairy-Related Contaminants. *J. Food Sci.* **2003**, *68*, 2788−2792.
(27) Li, J.; Zhuang, S. Antibacterial Activity of Chitosan and Its Derivatives and Their Interaction Mechanism with Bacteria: Current State and Perspectives. *Eur. Polym. J.* **2020**, *138*, No. 109984.
(28) Ospanova, A. K.; Savdenbekova, B. E.; Iskakova, M. K.; Omarova, R. A.; Zhartybaev, R. N.; Nussip, B. Z.; Abdikadyr, A. S. Obtaining Thin-Films Based on Chitosan and Carboxymethylcellulose with Antibacterial Properties for Biomedical Devices. *IOP Conf. Ser.: Mater. Sci. Eng.* **2017**, *230*, No. 012042.
(29) Liu, C.; Thormann, E.; Claesson, P. M.; Tyrode, E. Surface Grafted Chitosan Gels. Part I. Molecular Insight into the Formation of Chitosan and Poly(Acrylic Acid) Multilayers. *Langmuir* **2014**, *30*, 8866−8877.
(30) Bianchi, F.; Fornari, F.; Riboni, N.; Spadini, C.; Cabassi, C. S.; Iannarelli, M.; Carraro, C.; Mazzeo, P. P.; Bacchi, A.; Orlandini, S.; Furlanetto, S.; Careri, M. Development of Novel Cocrystal-Based Active Food Packaging by a Quality by Design Approach. *Food Chem.* **2021**, *347*, No. 129051.
(31) Coma, V.; Martial-Gros, A.; Garreau, S.; Copinet, A.; Salin, F.; Deschamps, A. Edible Antimicrobial Films Based on Chitosan Matrix. *J. Food Sci.* **2002**, *67*, 1162−1169.
(32) Boddohi, S.; Killingsworth, C. E.; Kipper, M. J. Polyelectrolyte Multilayer Assembly as a Function of PH and Ionic Strength Using the Polysaccharides Chitosan and Heparin. *Biomacromolecules* **2008**, *9*, 2021−2028.
(33) Bratskaya, S.; Marinin, D.; Simon, F.; Synytska, A.; Zschoche, S.; Busscher, H. J.; Jager, D.; van der Mei, H. C. Adhesion and Viability of Two Enterococcal Strains on Covalently Grafted Chitosan and Chitosan/κ-Carrageenan Multilayers. *Biomacromolecules* **2007**, *8*, 2960−2968.
(34) Ghavidel Mehr, N.; Hoemann, C. D.; Favis, B. D. Chitosan Surface Modification of Fully Interconnected 3D Porous Poly(ε-Caprolactone) by the LbL Approach. *Polymer* **2015**, *64*, 112−121.
(35) Gómez-Estaca, J.; Montero, P.; Giménez, B.; Gómez-Guillén, M. C. Effect of Functional Edible Films and High Pressure Processing on Microbial and Oxidative Spoilage in Cold-Smoked Sardine (Sardina Pilchardus). *Food Chem.* **2007**, *105*, 511−520.
(36) Ojagh, S. M.; Rezaei, M.; Razavi, S. H.; Hosseini, S. M. H. Development and Evaluation of a Novel Biodegradable Film Made from Chitosan and Cinnamon Essential Oil with Low Affinity toward Water. *Food Chem.* **2010**, *122*, 161−166.
(37) Dhurai, B.; Saraswathy, N.; Maheswaran, R.; Sethupathi, P.; Vanitha, P.; Vigneshwaran, S.; Rameshbabu, V. Electrospinning of Curcumin Loaded Chitosan/Poly (Lactic Acid) Nanofilm and Evaluation of Its Medicinal Characteristics. *Front. Mater. Sci.* **2013**, *7*, 350−361.
(38) Li, L.; Wang, X.; Li, D.; Qin, J.; Zhang, M.; Wang, K.; Zhao, J.; Zhang, L. LBL Deposition of Chitosan/Heparin Bilayers for Improving Biological Ability and Reducing Infection of Nanofibers. *Int. J. Biol. Macromol.* **2020**, *154*, 999−1006.
(39) Cazorla-Luna, R.; Martín-Illana, A.; Notario-Pérez, F.; Ruiz-Caro, R.; Veiga, M. D. Naturally Occurring Polyelectrolytes and Their Use for the Development of Complex-Based Mucoadhesive Drug Delivery Systems: An Overview. *Polymers* **2021**, *13*, 2241.

https://doi.org/10.1021/acsomega.3c02281
ACS Omega 2023, 8, 20031−20041

(40) Rezaei, F. S.; Sharifianjazi, F.; Esmaeilkhanian, A.; Salehi, E. Chitosan Films and Scaffolds for Regenerative Medicine Applications: A Review. *Carbohydr. Polym.* **2021**, *273*, No. 118631.
(41) Hu, B.; Guo, Y.; Li, H.; Liu, X.; Fu, Y.; Ding, F. Recent Advances in Chitosan-Based Layer-by-Layer Biomaterials and Their Biomedical Applications. *Carbohydr. Polym.* **2021**, *271*, No. 118427.
(42) Rahman, M. S.; Hasan, M. S.; Nitai, A. S.; Nam, S.; Karmakar, A. K.; Ahsan, M. S.; Shiddiky, M. J. A.; Ahmed, M. B. Recent Developments of Carboxymethyl Cellulose. *Polymers* **2021**, *13*, 1345.
(43) Liu, X.; Han, W.; Zhu, Y.; Xuan, H.; Ren, J.; Zhang, J.; Ge, L. Anti-Oxidative and Antibacterial Self-Healing Edible Polyelectrolyte Multilayer Film in Fresh-Cut Fruits. *J. Nanosci. Nanotechnol.* **2018**, *18*, 2592−2600.
(44) Yang, J.; Chen, Y.; Zhao, L.; Feng, Z.; Peng, K.; Wei, A.; Wang, Y.; Tong, Z.; Cheng, B. Preparation of a Chitosan/Carboxymethyl Chitosan/AgNPs Polyelectrolyte Composite Physical Hydrogel with Self-Healing Ability, Antibacterial Properties, and Good Biosafety Simultaneously, and Its Application as a Wound Dressing. *Composites, Part B* **2020**, *197*, No. 108139.
(45) Pérez-Álvarez, L.; Ruiz-Rubio, L.; Vilas-Vilela, J. L. Determining the Deacetylation Degree of Chitosan: Opportunities to Learn Instrumental Techniques. *J. Chem. Educ.* **2018**, *95*, 1022−1028.
(46) Jellison, G. E. Optical Functions of GaAs, GaP, and Ge Determined by Two-Channel Polarization Modulation Ellipsometry. *Opt. Mater.* **1992**, *1*, 151−160.
(47) Ciddor, P. E. Refractive Index of Air: New Equations for the Visible and near Infrared. *Appl. Opt.* **1996**, *35*, 1566−1573.
(48) Malitson, I. H. Interspecimen Comparison of the Refractive Index of Fused Silica. *J. Opt. Soc. Am.* **1965**, *55*, 1205−1209.
(49) Demadis, K. D.; Paspalaki, M.; Theodorou, J. Controlled Release of Bis (Phosphonate) Pharmaceuticals from Cationic Biodegradable Polymetic Matrices. *Ind. Eng. Chem. Res.* **2011**, *50*, 5873−5876.
(50) Park, J. W.; Choi, K. H.; Park, K. K. Acid-Base Equilibria and Related Properties of Chitosan. *Bull. Korean Chem. Soc.* **1983**, *4*, 68−72.
(51) Wüstenberg, T. Sodium Carboxymethylcellulose. In *Cellulose and Cellulose Derivatives in the Food Industry*; Wiley-VCG Verlag GmbH & Co. KGaA: Weinheim, 2014; pp 387−478, DOI: 10.1002/9783527682935.ch10.
(52) Li, L.; Srivastava, S.; Meng, S.; Ting, J. M.; Tirrell, M. V. Effects of Non-Electrostatic Intermolecular Interactions on the Phase Behavior of PH-Sensitive Polyelectrolyte Complexes. *Macromolecules* **2020**, *53*, 7835−7844.
(53) Quinn, J. F.; Johnston, A. P. R.; Such, G. K.; Zelikin, A. N.; Caruso, F. Next Generation, Sequentially Assembled Ultrathin Films: Beyond Electrostatics. *Chem. Soc. Rev.* **2007**, *36*, 707−718.
(54) Sham, A. Y. W.; Notley, S. M. Graphene-Polyelectrolyte Multilayer Film Formation Driven by Hydrogen Bonding. *J. Colloid Interface Sci.* **2015**, *456*, 32−41.
(55) Yang, S. Y.; Rubner, M. F. Micropatterning of Polymer Thin Films with PH-Sensitive and Cross-Linkable Hydrogen-Bonded Polyelectrolyte Multilayers. *J. Am. Chem. Soc.* **2002**, *124*, 2100−2101.
(56) Laschewsky, A.; Wischerhoff, E.; Denzinger, S.; Ringsdorf, H.; Delcorte, A.; Bertrand, P. Molecular Recognition by Hydrogen Bonding in Polyelectrolyte Multilayers. *Chem. - Eur. J.* **1997**, *3*, 34−38.
(57) Ferreira, D. C. M.; Ferreira, S. O.; de Alvarenga, E. S.; de Fátima Ferreira Soares, N.; dos Reis Coimbra, J. S.; de Oliveira, E. B. Polyelectrolyte Complexes (PECs) Obtained from Chitosan and Carboxymethylcellulose: A Physicochemical and Microstructural Study. *Carbohydr. Polym. Technol. Appl.* **2022**, *3*, No. 100197.
(58) Chen, P.; Xie, F.; Tang, F.; McNally, T. Glycerol Plasticisation of Chitosan/Carboxymethyl Cellulose Composites: Role of Interactions in Determining Structure and Properties. *Int. J. Biol. Macromol.* **2020**, *163*, 683−693.
(59) Chi, K.; Catchmark, J. M. Improved Eco-Friendly Barrier Materials Based on Crystalline Nanocellulose/Chitosan/Carboxymethyl Cellulose Polyelectrolyte Complexes. *Food Hydrocolloids* **2018**, *80*, 195−205.
(60) Bohinc, K.; Dražić, G.; Fink, R.; Oder, M.; Jevšnik, M.; Nipič, D.; Godič-Torkar, K.; Raspor, P. Available Surface Dictates Microbial Adhesion Capacity. *Int. J. Adhes. Adhes.* **2014**, *50*, 265−272.
(61) Ghostine, R. A.; Jisr, R. M.; Lehaf, A.; Schlenoff, J. B. Roughness and Salt Annealing in a Polyelectrolyte Multilayer. *Langmuir* **2013**, *29*, 11742−11750.

https://doi.org/10.1021/acsomega.3c02281
ACS Omega 2023, 8, 20031−20041